HHS Public Access

Author manuscript

Atherosclerosis. Author manuscript; available in PMC 2018 March 01.

Published in final edited form as:

Atherosclerosis. 2017 March ; 258: 20–25. doi:10.1016/j.atherosclerosis.2017.01.022.

Coronary atherosclerosis and dilation in hyper IgE syndrome patients: Depiction by magnetic resonance vessel wall imaging and pathological correlation

Khaled Z. Abd-Elmoniem[a], **Nadine Ramos**[a], **Saami K. Yazdani**[b], **Ahmed M. Ghanem**[a,c], **Steven M. Holland**[d], **Alexandra F. Freeman**[d], and **Ahmed M. Gharib**[a,*]

[a]National Institute of Diabetes and Digestive and Kidney Diseases, Biomedical and Metabolic Imaging Branch, United States

[b]University of South Alabama, United States

[c]Electrical Engineering Department, Suez Canal University, Ismailia, Egypt

[d]National Institute of Allergy and Infectious Diseases, United States

Abstract

Background and aims—Autosomal dominant hyper-IgE (AD-HIES) is a primary immunodeficiency caused by mutations in STAT3. Elevated levels of IgE, an ineffective immune response, connective tissue abnormalities, and coronary arterial dilation and tortuosity characterize AD-HIES. To date, coronary artery evaluation in AD-HIES patients has been limited to lumenography measurements. Direct *in vivo* coronary vessel wall (VW) imaging may allow for better interrogation of coronary vessel abnormalities. The goal of this prospective study was to evaluate the coronary VW of AD-HIES patients using Magnetic Resonance Imaging (MRI) and histology. VW image findings were compared in healthy subjects and subjects with coronary atherosclerotic disease (CAD).

Methods—A total of 28 subjects (10 with AD-HIES, 8 healthy, 10 with CAD) were studied by coronary VW MRI imaging. Additionally, a post-mortem coronary artery from one VW imaged AD-HIES patient was examined.

Results—Coronary VW in AD-HIES was thicker than in healthy controls but not significantly different from VW thickness in CAD subjects. AD-HIES coronaries showed increased VW area compared to healthy controls and CAD subjects. On histology, the AD-HIES coronary artery had findings consistent with atherosclerotic plaque, but had minimal luminal narrowing, deficient adventitia thickening and absence of both internal and external elastic laminae.

*Corresponding author. National Institutes of Health, Bldg. 10, CRC, Rm. 3-5340, United States. agharib@mail.nih.gov (A.M. Gharib).

Conflict of interest

The authors declared they do not have anything to disclose regarding conflict of interest with respect to this manuscript.

Author contributions

AMGharib, KZA, AFF and NR planned the study and wrote the draft. AMGharib and AMGhanem, NR, SY and KZA analyzed the data and edited the manuscript. SMH and AFF recruited and were involved in clinical aspects and performed critical revision of the manuscript.

Conclusions—This is the first study to demonstrate subclinical coronary atherosclerosis in AD-HIES patients on VW imaging by MRI. Histologic evaluation confirmed the presence of atherosclerosis with lack of supportive adventitial thickening and elastic components. These findings suggest mechanisms for coronary dilation in AD-HIES and thereby help direct clinical management.

Keywords

Autosomal dominant hyper-IgE (AD-HIES); Coronary vessel wall imaging; Coronary atherosclerotic disease; Coronary arterial dilation; Magnetic resonance imaging (MRI)

1. Introduction

Autosomal dominant hyper-IgE (AD-HIES) syndrome, also known as Job's syndrome, is a rare primary immunodeficiency caused by dominant negative mutations in STAT3 [1]. AD-HIES is characterized by elevated levels of IgE and ineffective immune response to specific infectious agents [2]. Additional clinical aspects of AD-HIES include eczema, recurrent skin and lung infections, as well as non-immune features such as a typical facial appearance as well as skeletal, connective tissue and arterial abnormalities [2,3].

Lumenography studies of coronary arteries lumen dimension in AD-HIES patients using computed tomography angiography (CTA) and magnetic resonance angiography (MRA) reveal marked increases in ectasia, aneurysms and tortuosity relative to control subjects [3,4]. These studies have hinted to the presence of mild atherosclerosis as depicted by mild stenosis or irregularities in the vessels [3,4]. This was fairly controversial as a large amount of atherosclerotic plaque burden, rather than such perceived paucity, is required to cause coronary artery ectasia and aneurysm [5,6].

Based on well-established relationships between lumen size and vessel wall thickness, angiographic data are used to infer vessel wall health [6,7]. While these relationships have held true in various populations, these data have not been reported for AD-HIES patients. To date, coronary artery evaluation in patients with AD-HIES has been limited to lumenography assessment and measurements using conventional angiography, CTA or MRA [3,4,8,9]. Therefore, we utilized a previously validated MRI technique [10,11] to directly measure the coronary artery vessel wall thickness (as a surrogate to subclinical atherosclerosis) in AD-HIES patients in comparison to non-AD-HIES patients with atherosclerosis and healthy controls.

Relative to lumenography, direct *in vivo* coronary vessel wall imaging may allow for earlier detection of coronary artery disease, possibly at the subclinical stage, and may lead to more accurate assessment of treatment effect [10,11]. Previous MRI techniques have been developed using 1.5 T scanners [12]. A free-breathing time-resolved dark-blood (TRAPD) MRI technique using a 3T scanner has improved upon those developed in 1.5 T scanners [11]. Specifically, TRAPD-MRI has a high temporal resolution, does not require a breath hold, and is less sensitive to patient variations in heart rate [11]. This technique is also more automated, with a high intraobserver, interobserver and interexperimentation reproducibility [11,13]. Additionally, the above are confirmed over a wide range of clinical coronary artery

disease [10,13] without the use of radiation, intravenous contrast agents or beta-blockers needed for CTA. Finally, although the vessel wall could be seen on CTA, this has been primarily performed by MRI [10–15] because of the better contrast between the vessel wall and suppressed luminal blood signal, as well as suppressed pericardial fat signal surrounding the vessel utilizing dual-inversion techniques; thus resulting in an enhanced ability to delineate the coronary vessel wall as the only positive signal contrasted against a suppressed lumen blood and outer fat signals on MRI. Contrariwise, on CTA it is usually difficult to reliably measure and quantify vessel wall thickness due to significant variability in tissue and injected luminal contrast densities as measured in Hounsfield Units (HU) [16]. Currently, the automatic segmentation methods have been primarily focused on measuring plaque volume at areas of minimal luminal narrowing [17], with limited application for subclinical atherosclerosis measurements of the coronary vessel wall as in this MRI method [10].

The goal of this prospective study was to directly evaluate the coronary artery vessel walls of AD-HIES patients using MRI in healthy subjects and those with known coronary artery disease. Additionally, histopathology was used to directly analyze the vessel wall and associated structures in one coronary artery from a patient with AD-HIES, who was previously imaged using the MR vessel wall imaging method.

2. Patients and methods

2.1. Subjects

A total of 28 subjects were included in this prospective case based study, which was approved by the local institutional review board (IRB). The study was conducted in compliance with the Declaration of Helsinki. All subjects signed informed consent before participation. The 10 subjects with AD-HIES had confirmed STAT3 mutations. The 10 patients with known CAD were confirmed by Coronary Computer Tomography Angiography (CTA). There were 8 healthy controls. The study is registered with clinicaltrials.gov as part of parent trail (NCT01399385).

2.2. Magnetic resonance imaging

MRI was performed in all 28 subjects and each session lasted between 35 and 55 min, including the following sequences:

2.2.1. Scout scanning—The beginning of the cardiac rest period was identified and anatomic slices, perpendicular to the proximal part of the right coronary artery (RCA) during diastole, were planned similar to a previously published method [12]. Patient-specific time delay between the R-wave of the electrocardiogram (ECG) and this rest period was used for the subsequent coronary MRA and wall imaging. This was followed by a fast 3D segmented k-space gradient-echo low resolution, navigator, and Vector ECG gated (VCG) wholeheart scan for localization of the coronaries. A pencil-beam navigator at the dome of the right hemidiaphragm, with an acceptance window of 8 mm, was used for tracking of respiratory motion and gating [18].

2.2.2. Phase-sensitive dual-inversion-recovery (DIR) coronary wall imaging— Single-slice free-breathing TRAPD coronary vessel wall datasets were acquired with a fixed inversion time (TI = 200 ms) and phase-sensitive reconstruction [11,14]. These imaging datasets were obtained in the proximal RCA segment, 1–3 cm distal to the vessel origin, at a location without noticeable stenosis or atherosclerotic disease on the coronary MRA image as previously described [10,11,13,14]. Data were acquired using a segmented k-space spiral acquisition (20 interleaves, acquisition window = 20 ms, $\alpha = 45°$) with spectral spatial excitation [19], using a 32-channel phased array cardiac received coil and VCG triggering [20]. Data from the 16 anterior surface coils were used for image reconstruction. Repetition time was 1 RR interval and the inplane spatial resolution was 0.69×0.69 mm^2 (field of view 200×200 mm^2, matrix 288×288). Data were acquired using prospective navigator-gating and correction [21].

2.2.3. Image data processing—Images were anonymized and blinded, zoomed to 500%, and the center of the vessel wall was manually traced as an initial localization step. Then, a one dimensional Gaussian-shape model was automatically fitted across the wall at all points along the wall's centerline. Outer and inner boundaries of the coronary wall were automatically identified as the two points of steepest gradients on the sides of each of the Gaussian shapes. Coronary artery wall thickness was measured as the average distance between identified inner and outer boundaries. Coronary luminal area and vessel wall area were also obtained for all subjects.

2.3. Coronary computed tomography angiography (CTA)

To confirm the presence of atherosclerosis, multidetector computerized tomography (MDCT) scans with electrocardiography (ECG) gating were performed in 10 CAD subjects. AD-HIES subjects had lung disease that would preclude the use of beta-blockers needed as preparation for MDCT. The MDCT protocol was similar to previously described techniques [8,22–24]. Briefly, between 30 and 60 min before MDCT, 50–100 mg of oral metoprolol was administered to achieve a target heart rate of approximately 65 beats per minute. This was performed using 70–80 ml of the non-ionic contrast iopamidol (Isovue, Bracco Diagnostic Inc, Princeton, NJ), which was injected through a peripheral intravenous 18–20 gauge catheter at a rate of 4–5 ml/s followed by 50 ml of 0.9% saline injected at the same rate. Image analysis and interpretation of the axial and the multiplanar reformatted images were performed using a three-dimensional software tool (Virtual Place, AZE, Tokyo Japan).

2.4. Pathology

2.4.1. Histological characterization of the coronary wall—Autopsy specimens of coronary arteries were taken from one AD-HIES 55-year old patient, less than 24 h after death and processed immediately. This patient was one of the AD-HIES patients imaged using the MRI method. She had a Framingham score of 1% due to her one coronary artery disease risk factor of hypertension. The cause of death was unclear, but there was no evidence of myocardial infarct, coronary artery embolism and/or rupture or plaque rupture. Routine hematoxylin and eosin staining and Movat special staining were performed on all samples to delineate connective tissue structures such as elastic fibers. Immunohistology was performed using antibody against CD-68 to identify macrophages. An internal scale was

used to allow for measurements. Details of methods are given in the Supplementary Materials.

2.5. Statistical analysis

For continuous variables, the mean ± standard deviation was used for summary statistics. These included age, body mass index (BMI), systolic and diastolic blood pressures, Framingham risk score (FRS) and coronary vessel wall thickness and luminal areas. Unadjusted comparison between the three groups was made using analysis of covariance (ANCOVA). Additional ANCOVA test for coronary luminal area, vessel wall thickness and vessel wall area was performed to adjust for the potential effect of age, followed by pairwise *t*-test. A Bonferroni-corrected $p < 0.05$ was considered statistically significant.

3. Results

3.1. Study population

All 28 subjects completed the MRI studies successfully and all 10 CAD subjects completed the coronary CTA studies. There was no statistical difference between BMI, blood pressure and FRS among the three groups. Table 1 displays the subjects' demographics and statistical difference.

3.1.1. Imaging—Six of the 10 AD-HIES subjects had either tortuosity and/or dilation of one of the coronary vessels. All CAD subjects had atherosclerosis in their coronary arteries as seen on coronary CTA. MRI imaging of coronary vessel walls of AD-HIES patients (1.4 mm (±0.2)) showed thicker vessel walls than those of healthy controls (n = 8; 1.1 mm (±0.1)) (Table 1 and Fig. 1). There was no statistically significant difference in vessel wall thickness between non-AD-HIES subjects with atherosclerosis (CAD subjects (1.3 mm (±0.2)) and AD-HIES patients (1.4 mm (±0.2)). The vessel wall area in AD-HIES (20.5 mm^2 (±10)) was significantly higher than both CAD (15.8 mm^2 (±4.3)) and healthy (13 mm^2 (±3)) subjects. The lumen area was significantly increased in AD-HIES (9.8 mm^2 (±9.7)) compared to CAD subjects (4.8 mm^2 (±2.5)) but not healthy controls (6.1 mm^2 (±4)).

3.1.2. Pathology—The left main coronary artery from the autopsy specimen showed vessel dilation at the bifurcation. The vessel wall was expanded and thickened by an atherosclerotic plaque, which occupied more than 60% of the vessel area (Fig. 2B). However, lumen stenosis was only 2.7%, relative to the reference section shown in Fig. 2A. Morphologic measurements were taken of the vessel wall as well. The wall thickness with adventitia was 1.36 mm. Vessel wall thickness without the adventitia was 1.14 mm and the thickness of the adventitia alone was 0.22 mm. Further histological assessment demonstrated an acellular region of the plaque with cholesterol clefts, consistent with a necrotic core (Fig. 2C). Morphological evaluation of the plaque site using the Movat stain showed thinning of both medial and adventitial layers relative to less affected areas of the vessel and absence of both internal and external elastic laminae, which should stain black with Movat staining when present (Fig. 2D). Additionally, inflammation is observed at the site of atherosclerotic

plaque, as evident by the heavy macrophage infiltration on the CD-68 immunohistochemistry stains (Fig. 2E).

4. Discussion

This is the first study to examine the coronary vessel wall of patients with AD-HIES both by non-invasive MR and histology. The MR vessel thickness in the cohort of AD-HIES patients was compared to both healthy subjects and patients with known coronary artery disease (CAD). The coronary vessel wall in AD-HIES subjects was significantly thicker than in healthy subjects, but comparable to patients with known CAD as demonstrated in Fig. 1 and Table 1. These findings suggest that the coronary arteries in AD-HIES do have atherosclerosis, consistent with the prevalence of aneurysms [3,4,8]. Postmortem histologic evaluation of a section of coronary artery from an AD-HIES patient confirmed the presence of atherosclerotic plaque (intimal medial thickening, macrophage infiltration, presence of foam cells, cholesterol clefts, etc.) (Fig. 2). Morphometric measurements also confirmed that the thickening was in the vessel wall proper, which measured 1.14 mm and not the adventitia, which measured 0.22 mm. When comparing our measurements to those cited by Hossain et al. [25], the vessel wall thickness of the coronary from the AD-HIES patient was more consistent with that found in CAD (0.98–1.0 mm) than healthy patients (0.46–0.5 mm). However, the adventitia in AD-HIES subject was considerably thinner than what Hossain et al. reported for healthy (0.54 mm) or diseased patients (0.92 mm), which would suggest that there is an altered healing/structure of atherosclerotic plaques in AD-HIES patients. These histologic and morphometric MRI findings support the hypothesis that wall thickening in coronary arteries of AD-HIES is actually associated with atherosclerotic plaque.

It is noteworthy that elastic laminae were conspicuously sparse in the region of the plaque of the AD-HIES coronary histology. This was demonstrated as absence of internal and external elastic laminae (absence of black stained tissue) on the movat pentachrom stain (Fig. 1D). Elastic laminae play crucial roles in maintaining the shape and structural integrity of the vessel wall. The loss of laminae would weaken the vessel wall, making it more susceptible to ectatic and aneurysmal changes. Prior studies of the coronary arteries in these subjects have primarily demonstrated ectasia, aneurysms and tortuosity of the coronary arteries [3,4,8]. However, these studies primarily utilized angiography, which is limited to lumenography measurement techniques that visualize the luminal diameter. Chandesris et al. [4] used carotid ultrasound to measure circumferential wall stress (CWS) and the intima-media thickness (IMT) in the common carotid arteries of subjects with AD-HIES syndrome. Although they reported mild but statistically significantly decreased IMT compared to healthy controls, the CWS was significantly increased in AD-HIES. This increased CWS usually results from an atherosclerotic process, which could have been underappreciated in this relatively younger age group. However, this was seen in our histological sample of a substantially older subject and reflected on the MRI coronary vessel wall images of the cohort. Chandesris et al. [4] did suggest the presence of atherosclerosis as evidenced by stenosis and irregularities in the coronary arteries as well as strokes and retinal occlusions. Those findings seem to affect medium sized vessels, such the coronary and intracranial cerebral vessels.

In this small, preliminary but prospective case based study, the clinical implications of coronary vessel wall thickening seen by MRI as a surrogate of subclinical atherosclerosis in AD-HIES were difficult to discern with confidence. However, despite the comparable coronary vessel wall thicknesses in the CAD and AD-HIES (1.3 mm *vs.* 1.4 mm), the average luminal area in CAD patients was 4.8 mm^2 compared to 9.8 mm^2 in AD-HIES, demonstrating a significantly larger lumen area in the latter ($p = 0.02$). Additionally, the vessel wall area was significantly larger in AD-HIES patients (20.5 mm^2) compared to both CAD patients (15.8 mm^2; $p = 0.006$) and healthy subjects (13 mm^2; $p = 0.03$). These VW measurements in the CAD patients and health subjects are in agreement with what was previously reported in the literature using comparable MRI methods [12]. Therefore, AD-HIES patients have an atherosclerotic plaque burden similar or more than that in CAD, which may result in vessel wall weakness, coronary artery ectasia and/or aneurysms. The enlarged coronary lumen in AD-HIES, compared to typical atherosclerosis in CAD patients (which results in narrowed lumens), may be the consequence of disorder in tissue remodeling associated with *STAT3* mutation. These patients have other manifestations of abnormal tissue remodeling, such as post-pneumonia pneumatoceles and impaired healing after lung surgeries [26]. This may in part be affected by abnormal regulation of matrix metalloproteinases (MMPs) [27]. MMPs are, in part, regulated by *STAT3*. MMP3, MMP8, and MMP9 plasma levels were found to be significantly different in AD-HIES samples compared to controls. MMPs are involved in vascular remodeling and dysregulation has been associated with abdominal aortic aneurysm and coronary artery ectasias [28]. Further studies will be necessary to determine the causality of atherosclerotic plaque burden in AD-HIES with ectasia, aneurysms and tortuosity.

Despite the relatively small number of patients, this preliminary but prospective case based report had enough statistical power to demonstrate the difference in coronary vessel wall thickness in AD-HIES compared to CAD and healthy controls. It is noteworthy that this number of AD-HIES subjects is substantial, given the rarity of this disease of unknown prevalence with only 200 cases described in the literature [29]. Histopathologic proof strengthens our interpretations of these results. However, we were limited by having only one patient with both imaging and histologic analysis and further studies will be necessary to determine the correlation of atherosclerotic plaque burden in AD-HIES with ectasia, aneurysms and tortuosity.

In conclusion, AD-HIES patients have significantly thicker coronary vessel walls than do healthy subjects, indicative of subclinical atherosclerosis. This vessel wall thickness is comparable to patients with known CAD. Additionally, AD-HIES coronary wall area is larger than CAD and healthy subjects. Pathological findings confirmed varying degrees of coronary atherosclerosis with impaired supportive structures, including advential thickening and elastic tissue proliferation. These findings by MR coronary vessel wall imaging and pathology offer a likely and consistent explanation for the ectasia and aneurysms seen in AD-HIES. This highlights the potential importance of managing modifiable risk factors for atherosclerosis in an effort to avoid the development of coronary abnormalities in AD-HIES.

Supplementary Material

Refer to Web version on PubMed Central for supplementary material.

Acknowledgments

Financial support

The study was financially supported as part of the National Institutes of Health (USA) intramural program for NIAID and NIDDK.

References

1. Minegishi Y, Saito M, Tsuchiya S, et al. Dominant-negative mutations in the DNA-binding domain of STAT3 cause hyper-IgE syndrome. Nature. 2007; 448:1058–1062. [PubMed: 17676033]
2. Sowerwine KJ, Holland SM, Freeman AF. Hyper-IgE syndrome update. Ann N Y Acad Sci. 2012; 1250:25–32. [PubMed: 22268731]
3. Freeman AF, Avila EM, Shaw PA, et al. Coronary artery abnormalities in Hyper-IgE syndrome. J Clin Immunol. 2011; 31:338–345. [PubMed: 21494893]
4. Chandesris MO, Azarine A, Ong KT, et al. Frequent and widespread vascular abnormalities in human signal transducer and activator of transcription 3 deficiency. Circ Cardiovasc Genet. 2012; 5:25–34. [PubMed: 22084479]
5. Pahlavan PS, Niroomand F. Coronary artery aneurysm: a review. Clin Cardiol. 2006; 29:439–443. [PubMed: 17063947]
6. Santos-Gallego CG, Picatoste B, Badimon JJ. Pathophysiology of acute coronary syndrome. Curr Atheroscler Rep. 2014; 16:401. [PubMed: 24504549]
7. Glagov S. Compensatory enlargement of human atherosclerotic coronary arteries. N Engl J Med. 1987; 316:1371–1375. [PubMed: 3574413]
8. Gharib AM, Pettigrew RI, Elagha A, et al. Coronary abnormalities in hyper-IgE recurrent infection syndrome: depiction at coronary MDCT angiography, AJR. Am J Roentgenol. 2009; 193:W478–W481. [PubMed: 19933621]
9. Ling JC, Freeman AF, Gharib AM, et al. Coronary artery aneurysms in patients with hyper IgE recurrent infection syndrome. Clin Immunol. 2007; 122:255–258. [PubMed: 17098478]
10. Abd-Elmoniem KZ, Unsal AB, Eshera S, et al. Increased coronary vessel wall thickness in HIV-infected young adults. Clin Infect Dis. 2014; 59:1779–1786. [PubMed: 25159580]
11. Abd-Elmoniem KZ, Gharib AM, Pettigrew RI. Coronary vessel wall 3-T MR imaging with time-resolved acquisition of phase-sensitive dual inversion-recovery (TRAPD) technique: initial results in patients with risk factors for coronary artery disease. Radiology. 2012; 265:715–723. [PubMed: 23047838]
12. Botnar RM, Stuber M, Kissinger KV, et al. Noninvasive coronary vessel wall and plaque imaging with magnetic resonance imaging. Circulation. 2000; 102:2582–2587. [PubMed: 11085960]
13. Gharib AM, Zahiri H, Matta J, et al. Feasibility of coronary artery wall thickening assessment in asymptomatic coronary artery disease using phase-sensitive dual-inversion recovery MRI at 3T. Magn Reson imaging. 2013; 31:1051–1058. [PubMed: 23642801]
14. Abd-Elmoniem KZ, Weiss RG, Stuber M. Phase-sensitive black-blood coronary vessel wall imaging, Magnetic resonance in medicine. Off J Soc Magn Reson Med/Soc Magn Reson Med. 2010; 63:1021–1030.
15. Di Carli, MF., Kwong, KF., editors. Novel Techniques for Imaging the Heart: Cardiac MR and CT. American Heart Association Willey-Blackwell; Dallas: 2008. p. 238
16. Ferencik M, Chan RC, Achenbach S, et al. Arterial wall imaging: evaluation with 16-section multidetector CT in blood vessel phantoms and ex vivo coronary arteries. Radiology. 2006; 240:708–716. [PubMed: 16857982]

17. Boogers MJ, Broersen A, van Velzen JE, et al. Automated quantification of coronary plaque with computed tomography: comparison with intravascular ultrasound using a dedicated registration algorithm for fusion-based quantification. Eur Heart J. 2012; 33:1007–1016. [PubMed: 22285583]
18. Stuber M, Botnar RM, Danias PG, et al. Double-oblique free-breathing high resolution three-dimensional coronary magnetic resonance angiography. J Am Coll Cardiol. 1999; 34:524–531. [PubMed: 10440168]
19. Meyer CH, Pauly JM, Macovski A, et al. Simultaneous spatial and spectral selective excitation, Magnetic resonance in medicine. Off J Soc Magn Reson Med/Soc Magn Reson Med. 1990; 15:287–304.
20. Fischer SE, Wickline SA, Lorenz CH. Novel real-time R-wave detection algorithm based on the vectorcardiogram for accurate gated magnetic resonance acquisitions, Magnetic resonance in medicine. Off J Soc Magn Reson Med/Soc Magn Reson Med. 1999; 42:361–370.
21. Danias PG, McConnell MV, Khasgiwala VC, et al. Prospective navigator correction of image position for coronary MR angiography. Radiology. 1997; 203:733–736. [PubMed: 9169696]
22. Garcia MJ, Lessick J, Hoffmann MH. Accuracy of 16-row multidetector computed tomography for the assessment of coronary artery stenosis. Jama. 2006; 296:403–411. [PubMed: 16868298]
23. Achenbach S, Moselewski F, Ropers D, et al. Detection of calcified and noncalcified coronary atherosclerotic plaque by contrast-enhanced, submillimeter multidetector spiral computed tomography: a segment-based comparison with intravascular ultrasound. Circulation. 2004; 109:14–17. [PubMed: 14691045]
24. Rybicki FJ, Otero HJ, Steigner ML, et al. Initial evaluation of coronary images from 320-detector row computed tomography. Int J Cardiovasc imaging. 2008; 24:535–546. [PubMed: 18368512]
25. Hossain SS, Hossainy SFA, Bazilevs Y, et al. Mathematical modeling of coupled drug and drug-encapsulated nanoparticle transport in patient-specific coronary artery walls. Comput Mech. 2011; 49:213–242.
26. Freeman AF, Renner ED, Henderson C, et al. Lung parenchyma surgery in autosomal dominant hyper-IgE syndrome. J Clin Immunol. 2013; 33:896–902. [PubMed: 23584561]
27. Sekhsaria V, Dodd LE, Hsu AP, et al. Plasma metalloproteinase levels are dysregulated in signal transducer and activator of transcription 3 mutated hyper-IgE syndrome. J Allergy Clin Immunol. 2011; 128:1124–1127. [PubMed: 21872914]
28. Morris DR, Biros E, Cronin O, et al. The association of genetic variants of matrix metalloproteinases with abdominal aortic aneurysm: a systematic review and meta-analysis. Heart. 2014; 100:295–302. [PubMed: 23813847]
29. Yong PF, Freeman AF, Engelhardt KR, et al. An update on the hyper-IgE syndromes. Arthritis Res Ther. 2012; 14:228. [PubMed: 23210525]

Appendix A. Supplementary data

Supplementary data related to this article can be found at http://dx.doi.org/10.1016/j.atherosclerosis.2017.01.022.

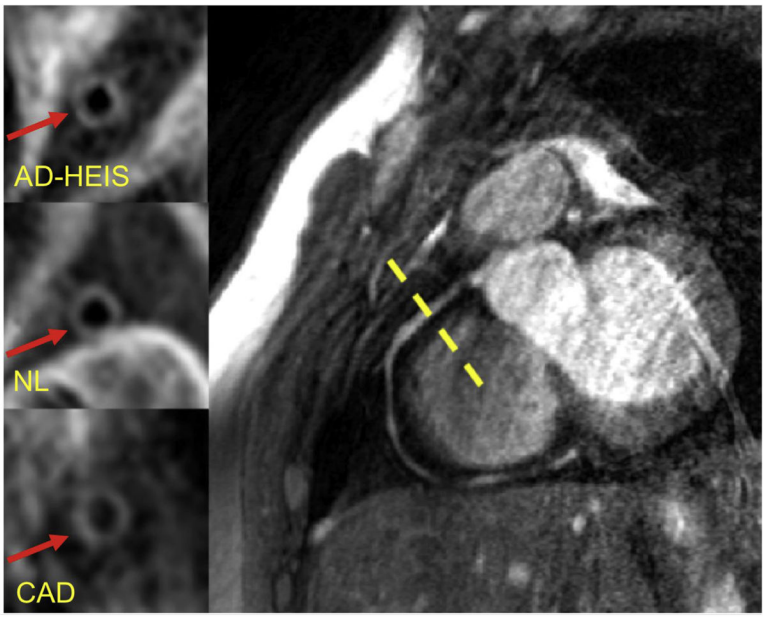

Fig. 1. Representative MR images of coronary vessel wall imaging

Example of right coronary artery 3T MRI image. Vessel wall image for one of the subjects in each of the three groups is shown in the left panels. AD-HIES, autosomal dominant hyper-IgE syndrome; NL, healthy subject; CAD, coronary artery disease.

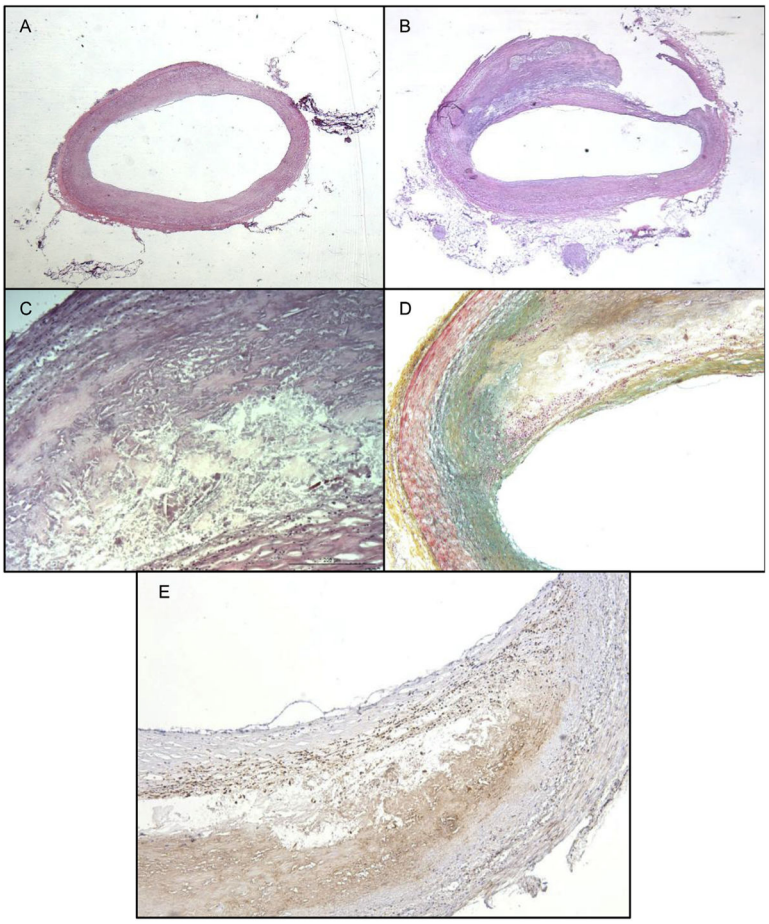

Fig. 2. Histological analysis of coronary artery in AD-HIES

(A) Section of artery adjacent to the affected area that is histologically normal. (B) Section of affected artery with plaque, showing several characteristics of atherosclerotic plaque better. (C) Higher magnification of plaque, showing intraplaque cholesterol clefts. (D) Absence of internal and external elastic laminae (absence of black stained tissue) in the region of the plaque. (E) Macrophage localization at plaque site indicating inflammation. A to E: hematoxylin & eosin staining. D: Movat pentachrome: Yellow: collagen and reticular fibers, blue: ground substance and mucin, red: muscle and red blood cells, black: elastic fibers, pink: cytoplasm. E: CD-68 immunohistology for macrophage labeling. (For interpretation of the references to colour in this figure legend, the reader is referred to the web version of this article.)

Table 1

Clinical characterization and MRI study results.

Summary (mean and standard deviation) of subject characteristics, vessel wall thickness, area and lumen area. Vessel wall thickness is significantly thicker in AD-HIES subjects compared to normal controls, but similar to subjects with known CAD. Vessel wall area in AD-HIES is significantly increased than both CAD and normal controls. Lumen area is significantly dilated in AD-HIES compared to CAD subjects but slightly larger than normal subjects (not statistically different).

	AD-HIES (n = 10)	CAD (n = 10)	Normal (n = 8)
Age (years)	31.1 (±15.4)	**47.3 (±13.4)** *	**29.5 (±9.3)** *
Framingham (%)	1 (1.8)	1.2(1.7)	0.5 (0.5)
Systolic BP (mmHg)	136 (±12.5)	125.5 (±14.9)	121 (±10.8)
Diastolic BP (mmHg)	72.0 (±11)	74.0 (±8)	72 (±6.3)
BMI (kg/m^2)	26.5 (±3.6)	26 (±2.8)	25 (±4.2)
Vessel wall thickness (mm)	**1.4 (±0.2)** *	1.3 (±0.2)	**1.1 (±0.1)** *
Vessel wall area (mm^2)	**20.5 (±10)** *▪	**15.8 (±4.3)** *	**13 (±3)**▪
Lumen area (mm^2)	**9.8 (±9.7)** *	**4.8 (±2.5)** *	6.1 (±4)

*▪ Bonferroni-corrected $p < 0.05$.